Geo-Mar Lett (2014) 34:483–498
DOI 10.1007/s00367-014-0379-x

ORIGINAL

Processes controlling very low sedimentation rates on the continental slope of the Gonone-Orosei canyon system, NE Sardinia—terrestrial and oceanic significance

Pierre Giresse · Vincenzo Pascucci · Gaël Lymer · Virginie Gaullier · Isabelle Thinon

Received: 27 December 2013 / Accepted: 21 July 2014 / Published online: 3 August 2014

Abstract The narrow shelf and upper slope immediately above the Gonone canyon head off NE Sardinia represent areas of very low sedimentation rates. Along the sides of the canyon head (1,600 m water depth), the sediment deposits are homogeneous but show alternating light-grey intervals rich in carbonate and dark-grey ones rich in organic matter, possibly related to distal turbidite processes. Deposits older than 50,000 years are already encountered at core depths of 2.50 m, the sedimentation rates varying from 6–21 cm/10^3 years in the lower parts of two cores and from 1.5–3 cm/10^3 years in the upper parts. At about 35,000 years BP, both cores show a simultaneous drop in sedimentation rate by a factor of 3, probably in response to local mechanisms of channel avulsion. Lithological, mineralogical and geochemical properties reveal the environmental factors which are responsible for the extremely slow sediment accumulation. The southernmost sector of the coast, and partly also of the shelf, consists of Jurassic limestones which supply only small amounts of fine-grained material transported in suspension. During the last sea-level highstand, the accumulation of the Cedrino River pro-delta remained restricted to the coast, the low siliciclastic sediment yields resulting in poor shelf sediment trapping. The present morphology of the canyon head prevented the occurrence of gravity processes in the deeper part of the canyon system, including the coring sites. Accordingly, deposition was mainly fed by hemipelagic material of planktonic origin, together with only moderate terrigenous inputs. On a wider late Pleistocene timescale, seismic data indicate the occurrence of a coarse-grained, layered turbidite facies, implying a very different architecture of the canyon drainage system probably prior to 60,000 years BP.

P. Giresse (✉)
Centre de Formation et de Recherche sur les Environnements Méditerranéens (CEFREM), UMR 5110 CNRS, Université de Perpignan Via Domitia, 52 av. Paul Alduy, 66860 Perpignan, France
e-mail: giresse@univ-perp.fr

V. Pascucci
Dipartimento di Architettura, Design e Urbanistica, Università degli Studi di Sassari, Via Piandanna 4, 07100 Sassari, Italy

G. Lymer · V. Gaullier
UMR 8217 CNRS Géosystèmes, Université de Lille 1, Cité scientifique - Bat. SN5, 59655 Villeneuve d'Ascq, France

I. Thinon
BRGM - Direction des Géoressources/GBS, BP 36009, 45060 Orléans Cedex, France

V. Pascucci
Institute of Geology and Petroleum Technologies, Kazan Federal University (Russian Federation), Kazan, Russia

Introduction

The Messinian event identified in the Tyrrhenian Sea on seismic records acquired in the course of the METYSS project serves to better constrain the relationships between crustal tectonics, salt tectonics and sedimentation along the eastern Sardinian continental margin during and after Messinian times. Besides revealing Messinian-age deposits, the high-resolution seismic profiles and sediment cores collected during successive METYSS cruises also made more recent sediments accessible. For the purpose of this study, the sediments of two cores recovered from the upper slope of the Gonone Canyon located along the eastern seaboard of Sardinian, as well as several surficial samples from the narrow shelf immediately above the canyon head, were analysed in detail. In this context, it is worth noting that the Gonone-Orosei canyon and submarine fan system is one of the largest natural gravity-induced accumulation areas along the east coast of Sardinia, in particular the bank ridges on the left flank of the Gonone Canyon (Dalla Valle 2007; Dalla Valle and Gamberi 2010).

In view of the fact that previous studies had noted a general dearth of siliciclastic sediments in the area, the purpose of the present study was to have a closer look at the lithological, mineralogical and geochemical characteristics of sediments from both the continental shelf and the Gonone Canyon with the aim of extracting information about the environmental factors which may have controlled local sediment supply and resulting sedimentation rates, these being among the lowest reported for the entire Mediterranean continental margin.

Geological and oceanographic setting

The Tyrrhenian basin formed from Miocene (Serravalian-Tortonian) to Quaternary times as a result of lithospheric stretching and thinning of the areas previously occupied by the Alpine-Apenninic orogens (Dewey et al. 1989; Patacca et al. 1990; Pascucci et al. 1999; Dalla Valle et al. 2013). The process of crustal thinning in the South Tyrrhenian domain was responsible for the formation of several small oceanic basins in the central Tyrrhenian Sea during the Pliocene and Quaternary (Mascle and Réhault 1990; Carminati et al. 1998; Sartori et al. 2001). Inland, this extensional tectonic activity has been relatively quiescent since the Early Pliocene and is characterized by minor rates of vertical movements (Antonioli et al. 1999; Ferranti et al. 2006). The locally uplifted Orosei area has been attributed to magmatic upwelling which resulted in the emplacement of the recent volcanic bodies in the region (Mariani et al. 2009). However, current investigations undertaken by the scientific team of the METYSS project have revealed that tectonic activity also affected the Orosei Gulf (east Sardinia, Figs. 1, 2) during the Pliocene (Chanier et al. 2011).

During the last glacial-interglacial cycle, the Mediterranean Sea was connected to the global ocean and therefore followed the same sea-level trends (Berné et al. 2007; Urgeles et al. 2011). The maximum sea-level lowstand in the Mediterranean is generally thought to have been at least 115 m below the present sea level (Jouet et al. 2006). During the deglacial, and especially after the Younger Dryas, the Mediterranean shows a constant sea-level rise. High-frequency sea-level fluctuations during the last highstand were minor as indicated by archaeological observations along the coast (Lambeck and Bard 2000; Lambeck et al. 2004).

Recent multibeam surveys have confirmed that the eastern margin of Sardinia, as in the case of Corsica (Pichevin et al. 2003), is characterized by deeply incised canyons originating from the small rivers (mostly ephemeral) which border the study area, and which can be followed down to the abyssal plain (Gamberi and Dalla Valle 2009; Pascucci et al. 2014). The Gonone-Orosei canyon system (Fig. 1) is a large submarine valley which cuts the entire upper Sardinian margin with a NW–SE trend. Its origin is probably associated either with instability processes following the uplift of the region because of early Pleistocene volcanic activity (Beccaluva et al. 1977, 1985; Carobene 1978; Lustrino et al. 2002) or with the Messinian Salinity Crisis (Lofi et al. 2011), or a combination of both. A previous side-scan sonar study did not reveal a lowstand link of the Gonone Canyon to the adjacent fluvial system (Martini et al. 2009). Instead, the canyon head has rough substrata outcrops, which testify to active retrogressive erosion. Muds on the upper slope show some obvious gravity-induced deformations of the creep-and-slump type in the direction of the central axis of the canyon (Pascucci et al. 2014).

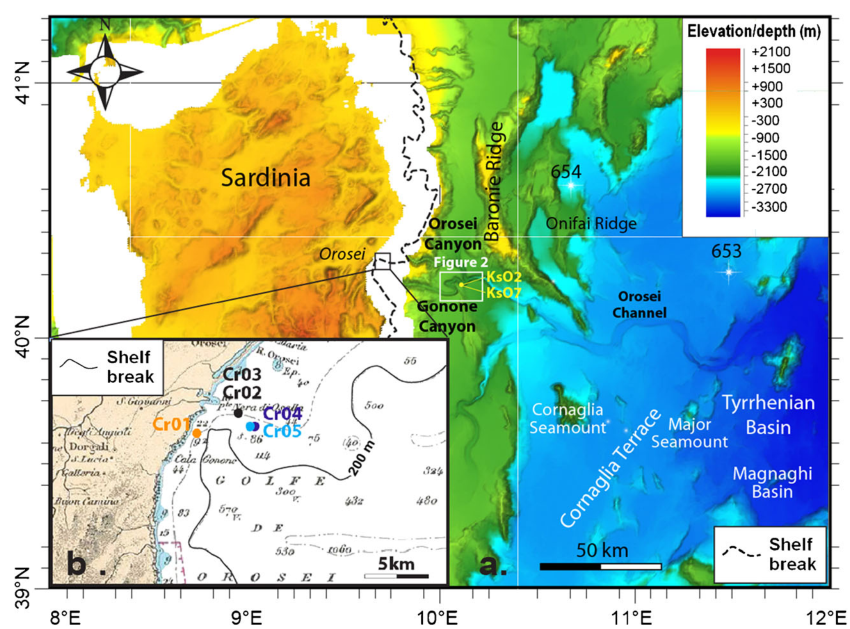

Fig. 1 **a** Colour-shaded bathymetric map of the study area (modified from CIESM/Ifremer Medimap Group 2008). *Black dashed line* Shelf break, i.e. 200 m isobath. **b** Bathymetric close-up showing the locations of the short cores on the continental shelf of the Orosei Gulf. See text for details

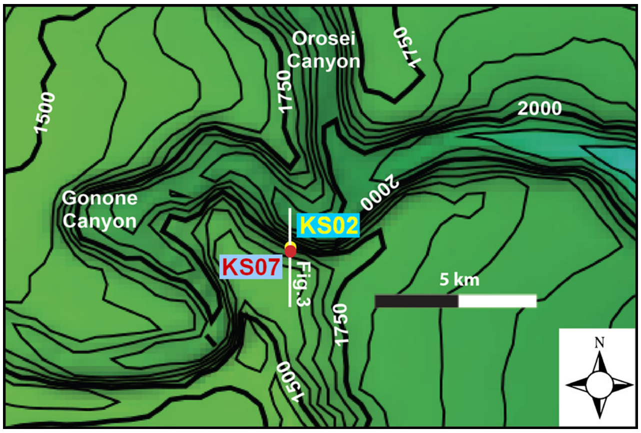

Fig. 2 Bathymetric close-up of the two piston core sites (KS02 and KS07) at the edge of the southern flank and upper slope of the Gonone Canyon. Isobath intervals: 50 m (map modified from CIESM/Ifremer Medimap Group 2008; for location, see Fig. 1). *White line* Location of the seismic line section shown in Fig. 3

The high-resolution seismic data acquired during the METYSS 1 cruise show three main sedimentary sequences commencing, respectively from bottom to top, with pre-MSC (Messinian Salinity Crisis), UU (late Messinian) and PQ (Plio-Quaternary) units (Fig. 3; Gaullier et al. 2014). The pre-MSC unit corresponds to high-energy deposition ranging from chaotic to roughly bedded reflectors. In Fig. 3, the strongly reflective, bedded seismic unit delineated by the dark (base) and light (top) green lines is attributed to the latest deposits of the MSC before the Pliocene reflooding (Upper Unit, using the recent seismic terminology established by Lofi et al. 2011). Above this MSC unit, the Plio-Quaternary series is divided into a weakly reflective to transparent basal unit, probably Early Pliocene in age, which is locally concordantly (purple line) overlain by a well-bedded reflective series of Late Pliocene to Quaternary age. This separation line corresponds to a regional seismic discontinuity observed in the whole study area which is elsewhere often associated with an angular unconformity attributed to a significant post-MSC deformation event (Gaullier et al. 2014). From a sedimentological point of view, the Plio-Quaternary unit is dominated by nannofossil and foraminiferal oozes as shown by ODP site 654 (Leg 107, Kastens et al. 1987; for location, see Fig. 1). The upper unit has been identified as representing late Messinian gypsum interbedded with clastic and dolomitic sediments.

The shelf is narrow and relatively steep, ranging in width from only 3–4 km with an average gradient of 3°, the width being reduced by half in front of the Gonone canyon head (Fig. 1). Especially in the inner part, rock outcrops consist of basalts, but also of Jurassic dolomitic limestones as, for example, encountered at a water depth of 50 m off Cala Luna (Pascucci et al. 2014). As a consequence, the continental shelf has a generally sediment-starved character linked to these conditions (for example, see Flemming 1981; Green 2009). A large part of the shelf between 5 and 35 m water depth is covered by marine phanerogam meadows, in particular *Cymodocea nodosa* on the landward and *Posidonia oceanica* on the seaward side, which proliferate especially on rocky outcrops. Posidoniaceae are responsible for the accumulation of so-called sediment banks (mattes) which reach heights of about 1.5 m. The lower shoreface is composed mainly of well-sorted bioclastic medium sand. Further offshore, the fine- to medium-grained deposits are mostly quartzose and feldspathic. The outer shelf is essentially composed of biogenic sands and gravels, followed by heterogeneous fine sands consisting of 50% bioclastic debris (Pascucci et al. 2014). A shallow-acoustic survey has indicated the existence of 20–30-m-thick deposits showing restricted progradation (Orrù and Ulzega 1987).

Between Santa Maria Navarrese in the south and the village of Cala Gonone in the north, the coast consists

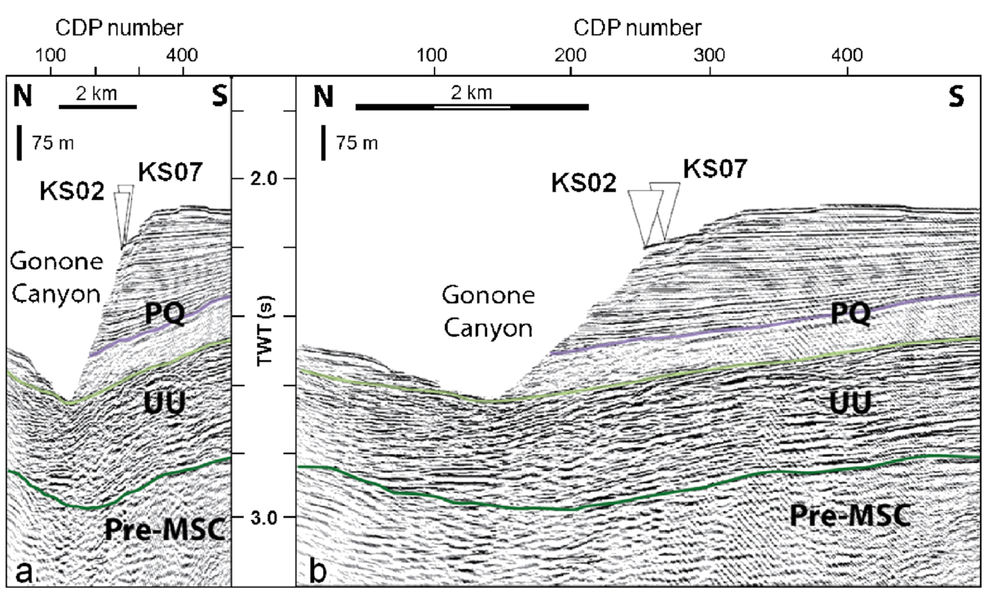

Fig. 3 Northernmost section of the MYS04d seismic line (METYSS 1 cruise of 2009; see Gaullier et al. 2014 for details) showing the locations of the KS02 and KS07 piston core sites. **a** Seismic section at 6× vertical exaggeration. **b** Seismic section at 2× vertical exaggeration. *Pre-MSC* Pre-Messinian Salinity Crisis sediment, *UU* upper unit, *PQ* Plio-Quaternary series. See text for details

of a 37-km-long succession of vertical Jurassic limestone cliffs reaching heights of 700 m. Further inland along the Cedrino valley, Hercynian granites and Palaeozoic sandstones and schists crop out. Several granitic hills are buried under Plio-Pleistocene basaltic lava flows.

The Cedrino River is the only perennial river of the region. There are no data on its present-day sediment discharge, the water flow being very irregular and subject to episodic catastrophic floods (Cossu et al. 2014).

Materials and methods

Within the framework of the METYSS project, the METYSS 1 cruise of 2009 onboard the R/V Téthys II-INSU collected seismic profiles along the upper and middle parts of the eastern Sardinian margin (Gaullier et al. 2014). The seismic sound source consisted of a mini-GI (SODERA) air gun and a 6-channel 25-m-long streamer. The profiles were processed using the Géovecteur software. During the subsequent METYSS 2 cruise in 2010, sediment samples were collected using a short corer (CNEXO-Ville) on the rocky continental shelf and a Kullenberg corer on the slopes of the Gonone-Orosei canyon system. A series of surficial samples (upper 10 cm) were collected with the CNEXO-Ville rock corer along a radial transect at 35, 38, 68, 70 and 248 m water depth, starting just seawards of the *Posidonia oceanica* meadow and ending at the top of the continental slope (Fig. 1b). Two longer sediment cores (KS02 and KS07) were recovered 200 m apart from the southern flank of the Gonone Canyon at 1,708 and 1,648 m water depth respectively (Figs. 1, 2).

The sediment cores were sampled at an average interval of 1 sample/10 cm, but this interval was shortened by a few centimetres depending on the colour (especially darker or lighter grey tones) and apparent textural changes. Samples were dried in the laboratory at 50 °C, water contents being determined from the weight loss. After wet-sieving at 63 and 315 µm, the two sand fractions were examined under a binocular microscope. Various tracers indicative of the last sea-level lowstand, such as iron-stained or altered debris originating from the outer shelf, were identified. The abundance of these particles are reported in terms of a 10-g sand fraction reference (>315 µm). Calcium carbonate contents were measured by means of a Bernard calcimeter.

Elemental distributions in <2 µm sub-fractions were determined at the Rock and Mineral Analysis Department of the CRP-CNRS, Vandœuvre, Nancy. The analyses were made by inductively coupled plasma optical emission spectrometry (ICP-OES Thermo Elemental IRIS radial) by applying total sediment digestion with $LiBO_2$ and HNO_3 (precision was <1% for SiO_2 and Al_2O_3, and <2% for the oxides). The ratio of two selected oxides was used to avoid dilution effects, Fe_2O_3/CaO ratios being particularly valuable for stratigraphic interpretations as Fe is considered to be of terrigenous origin and Ca mostly from marine calcareous tests. The Al_2O_3/CaO ratio served as an indicator of terrigenous input variability. Total organic contents, C and N in decarbonated <2 µm sub-fractions were measured by an Carlo Erba 1108 CHNS elemental analyser. The decision to use <2 µm sub-fractions for the analyses was taken to keep grain-size variations at a minimum in order to avoid confounding effects caused by the abundance of carbonates and siliciclastics in silt and sand fractions. For example, Al contents in marine sediments can generally be assigned to the fine-grained aluminosilicate detrital fraction (Calvert 1976).

Age datings were carried out by accelerator mass spectrometer (AMS) ^{14}C analyses at the Radiocarbon Laboratory in Posnan, Poland. Directly counting the number of ^{14}C and ^{12}C atoms requires smaller sample sizes and is more accurate than counting the decay activity of larger samples. The limit of measurability is approx. eight half-lives, or about 45,000 years. Larger samples were provided to extend the age range farther into the past. However, the error margin (±5,000 years) of two specific dates (45,000 and 50,000 years BP) implies that the true ages may lie outside the ranges listed in Table 1. Depending on the amount of material available to obtain 20-mg samples, the datings are mostly based on the single species *Orbulina* sp., occasionally complemented by *Globigerinoides bulloides* for some samples. Because the ages of numerous samples lay beyond 30,000 years BP, calibration into calendar years was not undertaken. To account for the reservoir effect, and as only few ^{14}C ages are available from Sardinian waters, the mean value for the western Mediterranean (400 years) was used for correction. In accordance with Imbrie et al. (1984), 11,000 years BP was chosen as the beginning of MIS (marine isotopic stage) 1, corresponding to the end of the Younger Dryas, 24,000 years BP for MIS II (near the LGM, last glacial maximum), 60,000 years BP for MIS III, and 71,000 years BP for MIS IV.

Results

Surficial sediments

Starting at the shoreline, the surficial bio- (*Posidonia* meadow) and sediment facies along the radial transect are illustrated in Fig. 4. Most of the facies consist of coarse-grained sands of ochre colour comprising blunt bioclasts of molluscs, bryozoans, sea urchin spines, *Lithothamnium* sp. and, more rarely, corals and *Posidonia* fibres; foraminifers are mainly represented by *Elphidium crispum*, *Ammonia beccarii* and various Miliolidae.

The sample collected at 240 m water depth is strongly heterogeneous and consists of coarse rounded quartz gravel, fragments of littoral fauna and black mottles of *Posidonia*

Table 1 Chronology of shelf biogenic deposits and of cores KS02 and KS07. Calibration into calendar years was not performed because most of the ages are older than 30,000 years BP. Note the paucity of radiocarbon reservoir data for the Sardinia margin. Holocene age constraints justify a 400-year reservoir age

	Water depth (m)	Latitude N	Longitude E	Matter	Lab. no.	Conventional ^{14}C age (years BP)
Grab sample no.						
Cr031/2	38	40°19.08′	9°42.92′	Bittium	Poz-37944	1,820±30
Cr032/2	38	40°19.08′	9°42.92′	Lithothamnium	Poz-37945	2,355±30
Cr042/2	68	40°18.59′	9°43.63′	Bittium	Poz-37946	1,785±30
Cr051/2	70	40°18.58′	9°43.58′	Bittium	Poz-37947	2,440±30
Cr01	248	40°18.26′	9°40.49′	Bittium	Poz-37943	1,935±30
Core no.						
KS02, 106–110 cm	1,602	40°12.45′	10°6.58′	Pelagic foraminifers	Poz-38825	36,900±1,200
KS02, 191–200 cm					Poz-38826	>46,000
KS02, 276 cm					Poz-37940	52,000±4,000
KS07, 6–12 cm	1,648	40°12.44′	10°6.54′	Pelagic foraminifers	Poz-42575	8,870±50
KS07, 37–46 cm					Poz-38829	30,300±500
KS07, 92–98 cm					Poz-38828	38,800±1,200
KS07, 125–135 cm					Poz-38827	43,600±2,200
KS07, 143–154 cm					Poz-42573	45,000±5,000
KS07, 219–227 cm					Poz-38828	50,000±5,000
KS07, 234–240 cm					Poz-42574	>54,000

matte origin. Quartz clasts are similar to those commonly found on the Pleistocene terraces of the Cedrino River valley, and these are abundant also on the beaches close to its present mouth (Chanier et al. 2011; Giresse et al. 2011).

Five AMS ^{14}C dates were obtained from tests of the predatory gastropod *Bittium reticulatum* because it occurred in all samples, the datings being carried out on the non-recrystallized aragonite shell sections. In addition, a date was obtained from a concretion of *Lithothamnium calcareum* collected in 38 m water depth. All ages are well grouped between 1,820 and 2,440 years BP (i.e. 2,220–2,840 years BP when taking the correction of the 400-year reservoir effect into account; Table 1).

Sediment cores KS02 and KS07

Main lithofacies

The two sediment cores (KS02 and KS07), which were taken approx. 200 m apart in only marginally different water depths (60 m difference), consist of homogeneous grey muds, except near the summit where the oxidated surface layer was 15 cm thick in core KS07 and 57 cm thick in core KS02. Both cores are composed of rather similar lithologic successions (Fig. 5). The examination of photographs taken from the split-core sections revealed a succession of lighter and darker grey intervals, which are especially well developed in core KS02.

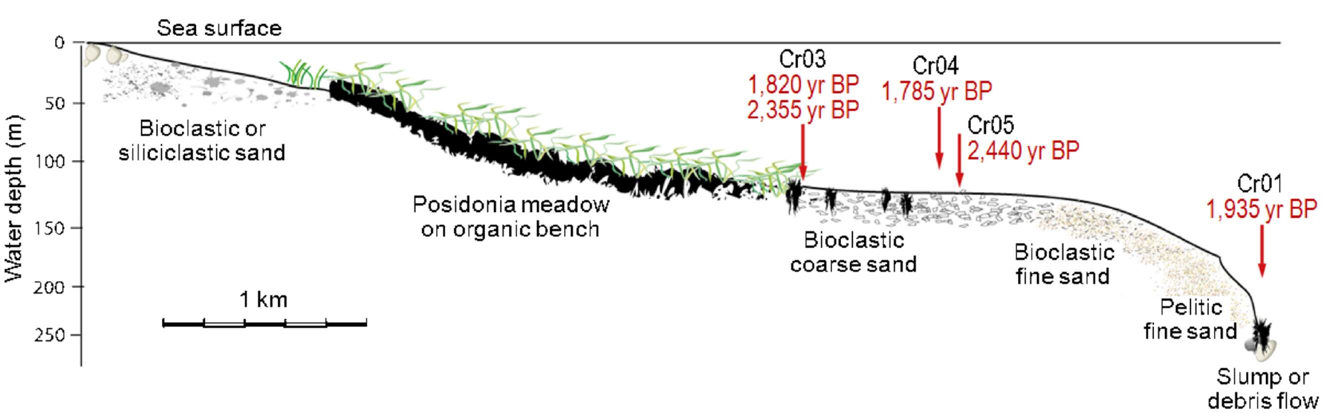

Fig. 4 Schematic succession of sedimentary facies observed on the narrow shelf above the Gonone Canyon together with the locations of ^{14}C AMS dated sediments

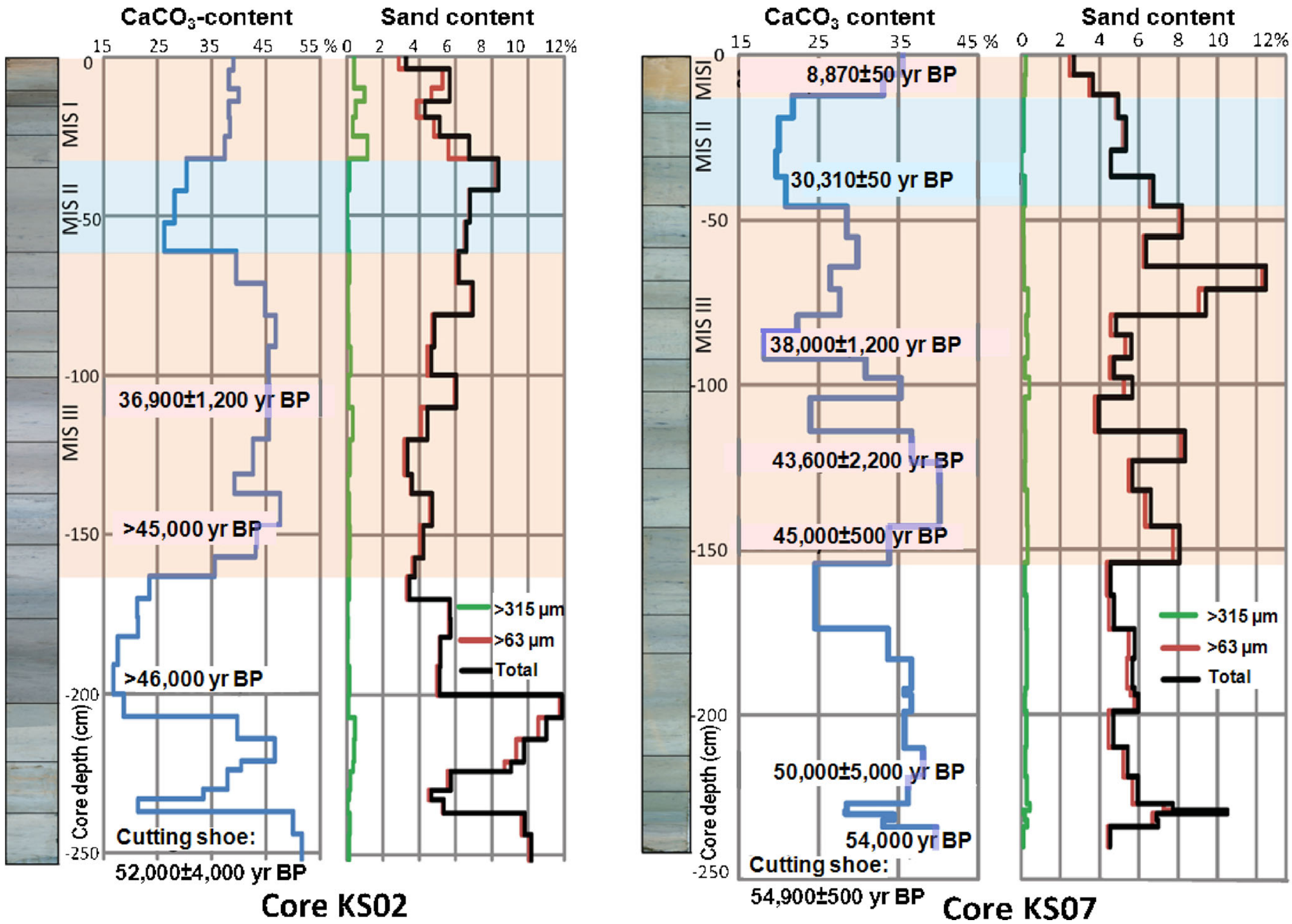

Fig. 5 Lithological logs of cores KS02 and KS07, together with $CaCO_3$ and sand contents

The lighter grey episodes are richer in carbonate and sometimes slightly speckled with black spots of organic matter and iron monosulphides, whereas the darker-grey or grey-brown intervals, where the mud is somewhat richer in organic matter, are sometimes laminated in the form of sub-millimetre-thick microlaminae (especially between 2.3 and 1.7 m depths in core KS02).

The low sand fractions (4–12% of the total sediment) are often entirely composed of pelagic microfaunal tests. Accordingly, the rather variable carbonate contents (15–45%) turn out to be mostly representative of the sand fractions. Only core KS07 shows some faint centimetre-scale microbedding (Fig. 6) near the bottom.

Downcore bio- and lithological markers

The biogenic and lithological compositions of the two cores are illustrated in Fig. 7. In core KS02, the sand fraction consists mainly of planktonic foraminifers. Benthic foraminifers (*Elphidium crispum*, *Ammonia beccarii*) or blunt and oxidized bioclasts, or even glauconitic grains which may constitute markers of gravity transfer from the shelf, were not found in this core. Pteropod debris occur only locally and form a subordinate component in some more carbonate-rich intervals but do not contribute substantially to the mass of the grain-size fractions. The same applies to the remains (spines, stereomes) of mud-eating echinoids, which represent the benthic production here. Finally, although occurring throughout the core, fish otoliths play an overall negligible role.

The sand fractions of core KS02 contain only small numbers of quartz grains, the largest being just under 500 µm in size. The vertical distribution of these grains does not reveal any characteristic pattern. On the other hand, other indicators of gravity transfer such as oxidized rock fragments occur rather frequently and are particularly abundant in the 30–60 cm core depth interval. Fragments and plaques of a dark-grey Jurassic limestone constitute a characteristic marker, especially at about 25, 110–130, 190 and 220 cm core depths. These fragments often have white carbonate coatings or films precipitated from supersaturated littoral waters of the last sea-level lowstand (Fig. 8). The rock fragments also provide evidence for authigenic pyrite formations, which invariably mask the grey limestone and its white coating.

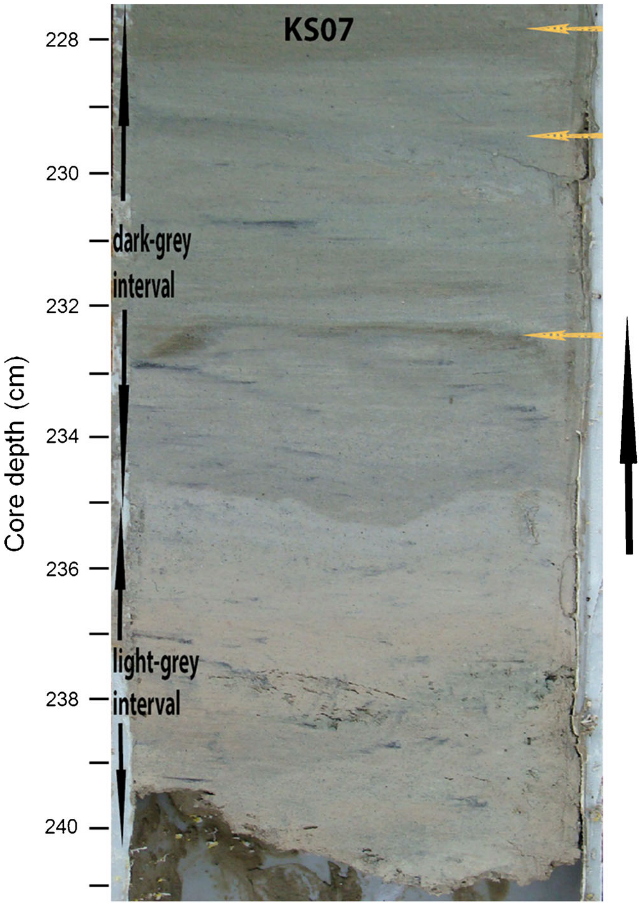

Fig. 6 Bottom section of core KS07 (core length: 2.4 m) with evidence of centimetre-thick distal microturbidites (*yellow arrows*)

Some black plant fragments (occasionally carbonized) are observed locally at about 20, 110–120, 220 and 240 cm core depths, sometimes coinciding with the occurrence of the limestone fragments. As will be seen below, these layers also coincide with higher organic carbon contents.

In both cores, planktonic foraminifers constitute the main part of the sand fractions. Other biogenic components, such as pteropod fragments, are more irregularly distributed, the calcareous benthos being represented by the remains of mud-dwelling sea urchins (spines and stereomes) which seem to be ubiquitous throughout the sediment. Fish otoliths are notably observed at core depths of about 160, 110 and 35 cm.

As in core KS02, quartz grains are very scarce throughout core KS07, generally not exceeding two grains per 10 g sand in the >315 μm fraction. Their distribution does not show any vertical trend, the diameter of the coarsest grains ranging from 100–400 μm. The only remarkable marker is constituted by oxidized fragments which are observed in the upper 30 cm of the core, especially from 20–30 cm. The more or less carbonized black fragments and fragments of limestone observed in KS02 were not encountered in core KS07.

^{14}C age datings and sediment accumulation rates

A coherent succession of eight age datings are available from core KS07, starting at 54,900±5,000 years BP for the sediment in the cutting shoe and ending at 8,870 years BP at approx. 10 cm core depth; thus MIS I, MIS II and MIS III, and probably the upper part of MIS IV, are successively crossed (Figs. 5, 9, Table 1). Due to inadequate quantities of carbonate, two indefinite ages beyond 46,000 and 52,000 years BP were obtained from core KS02 (Fig. 5). The other two dates, 52,000±4,000 and 36,900±1,200 years BP, are located at almost the same core depth as those of core KS07, indicating that the two cores have a very similar chronostratigraphy (Figs. 5, 9).

The sedimentation rates determined for the two cores are extremely low, this being emphasized by the fact that ages exceeding 50,000 years BP were already encountered at core depths of only about 2.50 m. The sedimentation rates of both cores initially range from 6–21 cm/10^3 years between 50,000 and 30,000 years BP up to core depths of 30 cm in core KS07 and about 1 m in core KS02, before decreasing strongly to only 1.5–3 cm/10^3 years in the core sections above those depths (Fig. 9). In effect, this means that the sedimentation rates in both cores are essentially identical over the last 50 millennia, which is not unexpected considering their close spacing and similar water depths. However, some differences are evident on the scale of successive palaeoclimatic intervals represented by successive marine isotope stages.

In core KS07, the Holocene accumulation amounts to only 15 cm (corresponding to the ochre levels above the redoxcline), whereas in core KS02 the same interval is represented by approx. 35 cm. The accumulation rate ratios of the two cores are thus inverted during MIS 2, while they are approx. equivalent during MIS 3. On the basis of the time intervals determined by the ^{14}C AMS datings, the average period between dark-grey and light-grey sedimentary sequences amounts to 3,500 years for core KS02 and 4,150 years for core KS07, i.e. a difference of 650 years despite their spatial proximity.

Geochemistry of the <2 μm fraction

In core KS02, aluminium (ranging from 6.3–14.8%) and iron (2.5–5.6%) represent two major elements of terrigenous supply (Fig. 10). Iron oxides have not been detected in any of the samples and pyrite aggregates are restricted to the sand fraction. The vertical trends of Al_2O_3/CaO and Fe_2O_3/CaO ratios are almost identical and opposed to the carbonate accumulation trend, which is mainly of planktonic origin. The small variations in the MgO/Al_2O_3 ratios underline episodes of stronger biogenic accumulation. The same applies to the P_2O_5 contents (0.10–0.21%). The contents of all other major

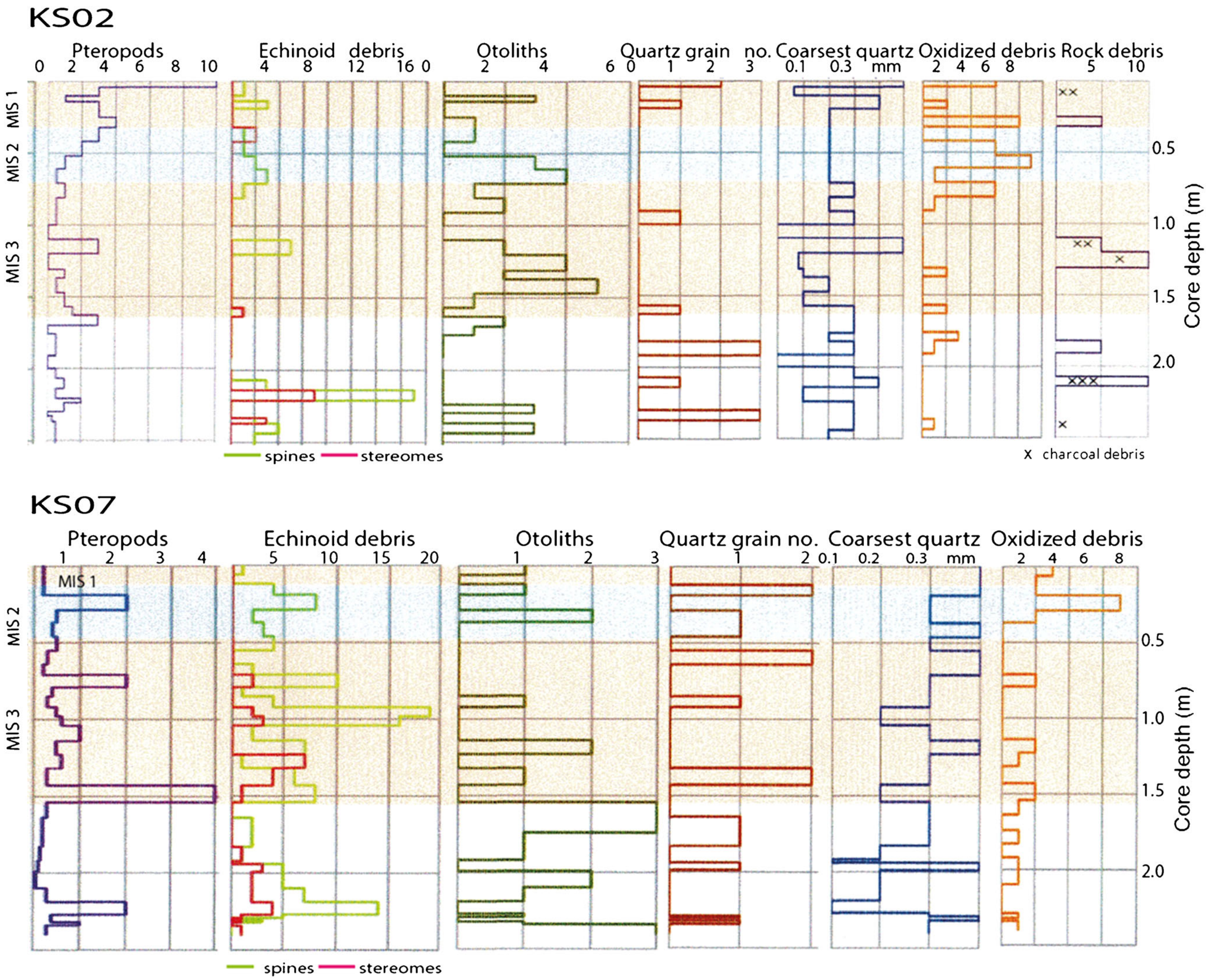

Fig. 7 Additional sedimentary components and biomarkers of cores KS02 and KS07

elements confirm the relatively constant nature of the terrigenous supply. Titanium, in particular, shows little variations in content, the major elements as a whole being independent of the other constituents.

The organic carbon contents vary from 0.5–2.5%, with occasional peaks of 3 and even 4%. Maximum values are invariably associated with the darkest beds of the sedimentary column, being associated with the presence of some quartz grains, and oxidized rock and plant fragments. In all beds showing high organic matter contents, the C/N ratios are higher than 20, and occasionally reach 30 or 40.

As in the case of core KS02, the aluminium (ranging from 9.1–15.3%) and iron (3.3–6.2%) contents in core KS07 constitute the two main elements in the sediments (Fig. 11), the Al_2O_3/CaO and Fe_2O_3/CaO ratios showing similar vertical trends in opposition to that of the carbonate content, which is again underlined by maximum MgO/Al_2O_3 ratios. The P_2O_5 contents, although rather constant (0.12–0.17%), correspond to the maxima of planktonic carbonate accumulation. The contents of the other elements, both major and minor, do not show any significant vertical variation.

The organic carbon contents, for the main part, range from 0.5–2% and only reach peaks of up to 2.5% in the dark layers marking the lower part of the core. As a consequence, the colour contrasts to the terrigenous dark-grey beds are a little less obvious. All the Corg maxima correspond to maxima of the C/N ratio (>15). However, as the Corg contents in core KS02 are on the whole lower than in KS07, the C/N maxima in core KS07 do not exceed 20, with the exception once again of the lowermost beds of the core. The black debris observed in core KS02 are too rare to be accurately quantified, only the oxidized debris providing occasional evidence for effective downslope processes (i.e. core depths of ca. 1.80, 1.50, 0.75 and especially 0.3–0.2 m). As in core KS02, the relative contents of terrigenous organic matter in core KS07 are

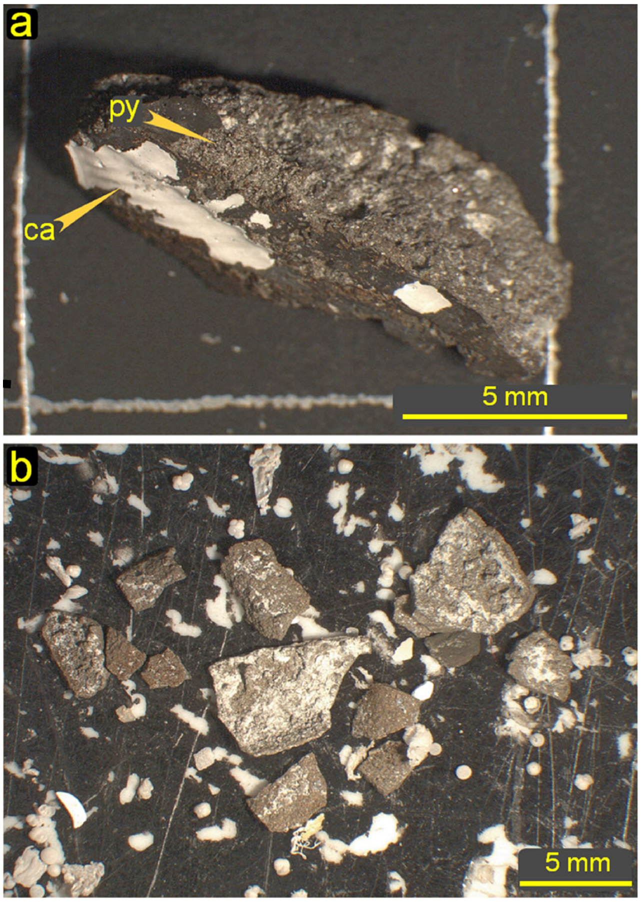

Fig. 8 **a** Jurassic limestone debris coated by a white calcite film (*ca*) and by pyrite (*py*). **b** Assemblage of allochthonous Jurassic debris originating from the shelf edge

independent of the MIS 2, 3 and 4 chronology, even if they are slightly less obvious. In both cores, the supply of organic matter is not closely connected to that of the siliciclastic component.

Discussion

General aspects of shelf and slope deposition

On the inner shelf, fine-grained quartzose and feldspathic sediments are dispersed by long-shore drift and wave action, the largest source being the Cedrino River. Quartz clasts are similar to those commonly found on the nearby Pleistocene terraces of the Cedrino River valley, and are most abundant on the beaches close to its mouth (Chanier et al. 2011; Giresse et al. 2011). However, the prevailing sedimentation on the shelf is predominantly of biogenic origin. Today, the low concentration of fine-grained terrigenous matter in the shelf waters favours transparency and hence high macroalgal productivity (in particular by *Cymodocea nodosa*, *Posidonia oceanica* and *Lithothamnium*) which completely masks the relict lowstand deposits. The latter are frequently observed in outcrop along most of the shelf breaks of the Mediterranean (Leclaire 1972; Palanques et al. 2002; Giresse et al. 2009; Lo Iacono et al. 2010). Ages between 1,820 and 2,440 years BP indicate high biogenic carbonate production during stable highstand periods, which suggests the existence of optimal oceanic conditions. This biological activity is probably concomitant with the development of *Posidonia oceanica* meadows.

The heterogeneous composition of the deposits in 240 m water depth suggests formation by a debris flow encompassing a rather large area of the shelf break, thus confirming previous assumptions about slope instability around the canyon heads (Martini et al. 2009). These gravity processes are of young age, having probably occurred after the last sea-level highstand.

Both upper slope cores reflect rather similar depositional processes governed by slow sedimentation, the rate being about three times lower than that observed on the Algerian

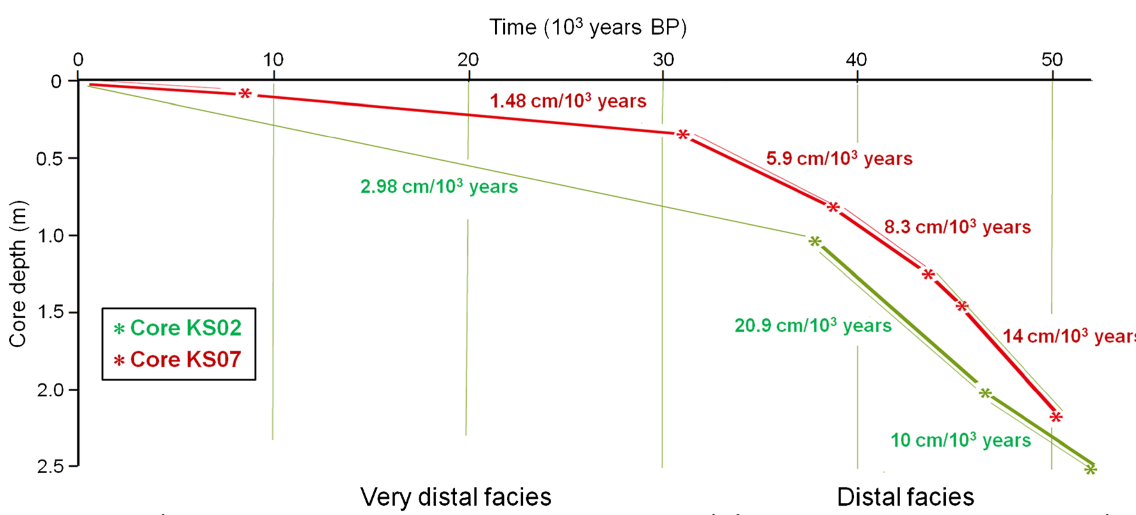

Fig. 9 Comparison of sediment accumulation rates of cores KS02 and KS07

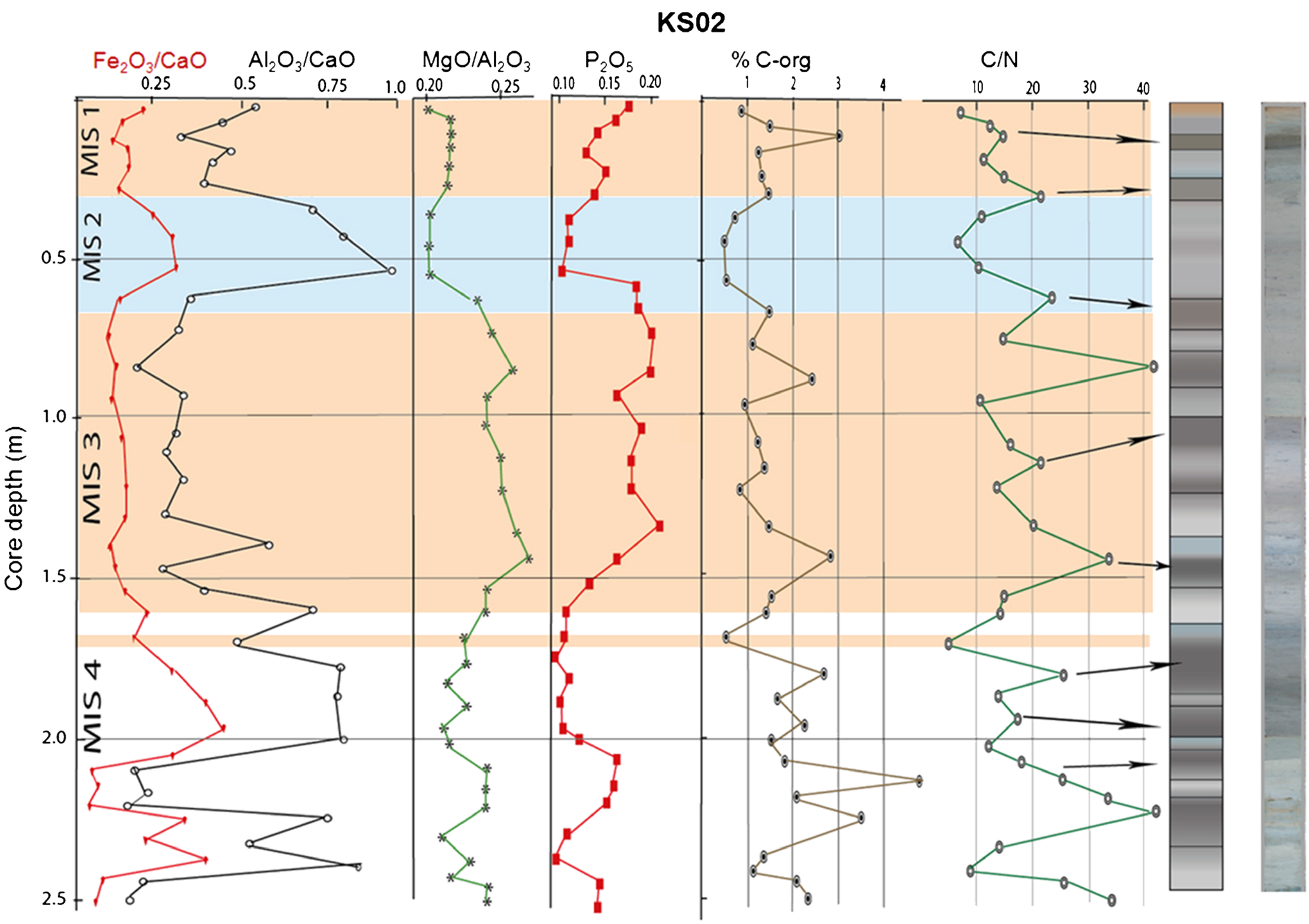

Fig. 10 Core KS02 downcore profiles of Al_2O_3/CaO, MgO/Al_2O_3, Fe_2O_3/CaO and C/N ratios as well as P_2O_5 and organic carbon (Corg) contents, together with the core log; C/N peaks are correlated with dark grey intervals (*arrows*)

side of the Mediterranean (core KMDJ38) which to date was considered as one of the lowest of the Mediterranean margins (Giresse et al. 2009, 2013). In the present case, the lowest carbonate contents in both cores are about 15%, whereas the highest approach 50% in core KS02 and 40% in core KS07. The latter are among the highest $CaCO_3$ contents recorded in hemipelagic sediments on Mediterranean continental slopes. For comparison, the carbonate contents along the Algerian margin range from 20–35% (Giresse et al. 2009).

The occurrence of fish otoliths is usually related to periods of colder waters associated with higher oceanic productivity. Such events recurred quite frequently during the last 60,000 years and only some of the carbonate peaks would thus be related to the LGM, and possibly also to MIS III (cf. Fig. 5, core KS02) or MIS IV (Fig. 5, core KS07).

To explain the very low sedimentation rates, one could envisage erosion (planation) of the uppermost parts of the deposits at the coring sites but, at this stage of the investigation, there is no evidence that such truncation took place. Slight differences in sedimentation rates between the two cores suggest that, in spite of their proximity, the small terrigenous inputs at the two sites varied slightly in space and time.

The deposition of the sediments at the coring sites must have occurred after the seabed geometry produced by the main slope-failure event was modified by subsequent, more localized gravity processes (Figs. 7, 12). These morphological modifications must have taken place before 50,000 years BP, probably in the period between 100,000 and 60,000 years BP. This would mean that the reduction in sedimentation rates recorded at the two coring sites before 35,000 years BP document a growing isolation from the influence of gravity processes. One must thus assume that both the original canyon head valley and its upstream feeder channel changed their position and orientation. The previous path of the turbidity currents probably followed a more deeply incised valley, at the time possibly still aligned more obliquely to the shelf break. The evidence of some obvious gravity-induced deformations of the creep-and-slump type in the direction of the central axis of the canyon (Pascucci et al. 2014) may actually reflect this morphological change.

In depositional terms, this can be envisaged as the passage from a proximal to a distal turbidite facies at the coring sites

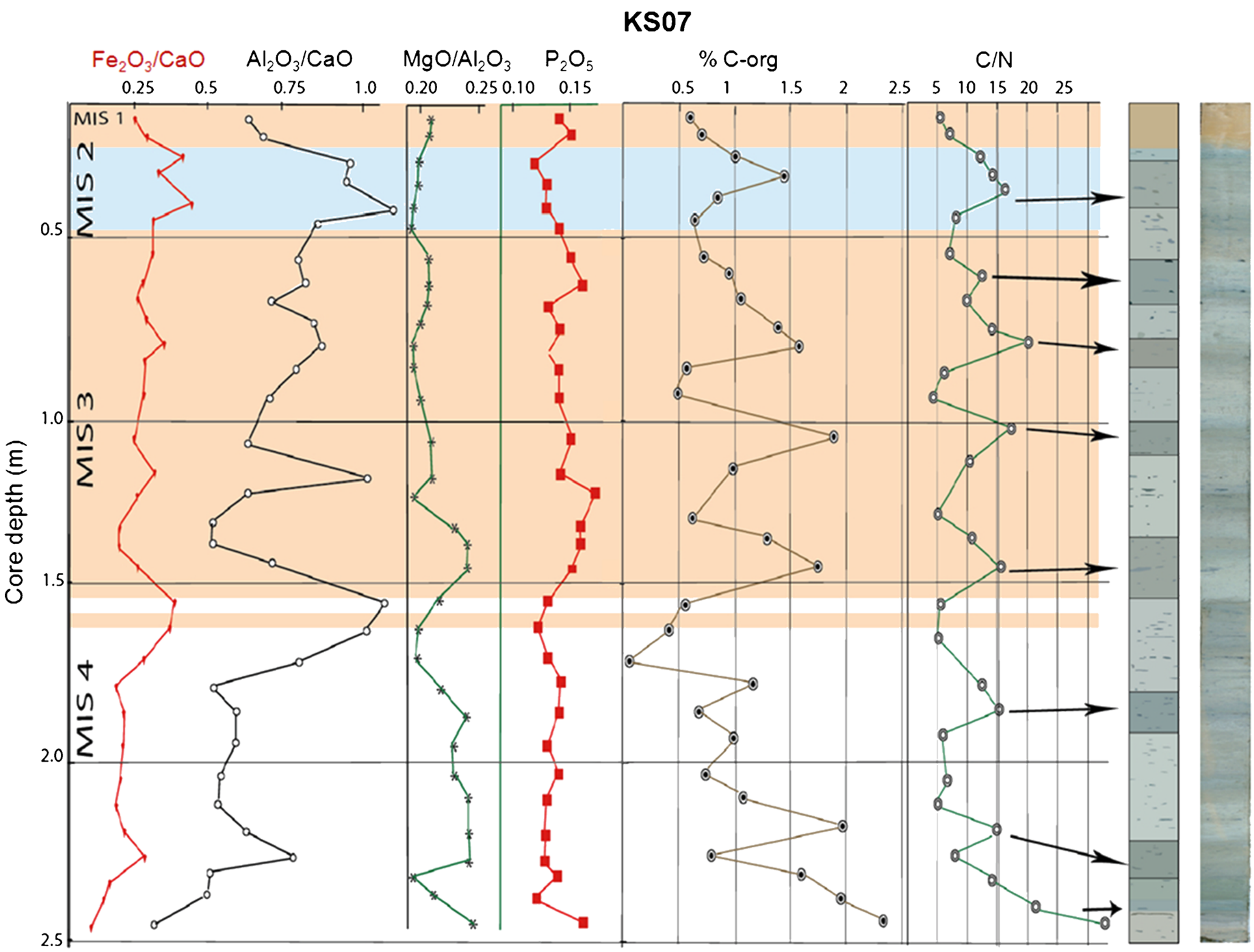

Fig. 11 Core KS07 downcore profiles of Al_2O_3/CaO, MgO/Al_2O_3, Fe_2O_3/CaO, C/N ratios as well as P_2O_5 and organic carbon (Corg) contents, together with the core log; C/N peaks are correlated with dark grey intervals (*arrows*)

(Fig. 12). Indeed, the deposition of recurrent darker-grey and lighter-grey successions in the course of the last 50,000 years is highly suggestive of a distal turbidite facies. Discrete markers of gravity process are represented by oxidized rock

Fig. 12 Schematic model of the sedimentation trend on the upper slope of the Gonone Canyon based on the KS02 and KS07 cores covering the last 50,000 years, and according to seismic data for the older Pleistocene. The accumulation rates of turbidites marked by an asterisk (*) are the range proposed by Wetzel (1984), Droxler and Schlager (1985) and Grantz et al. (1996). Note the factor of more than 10 lower rates for the Sardinian margin

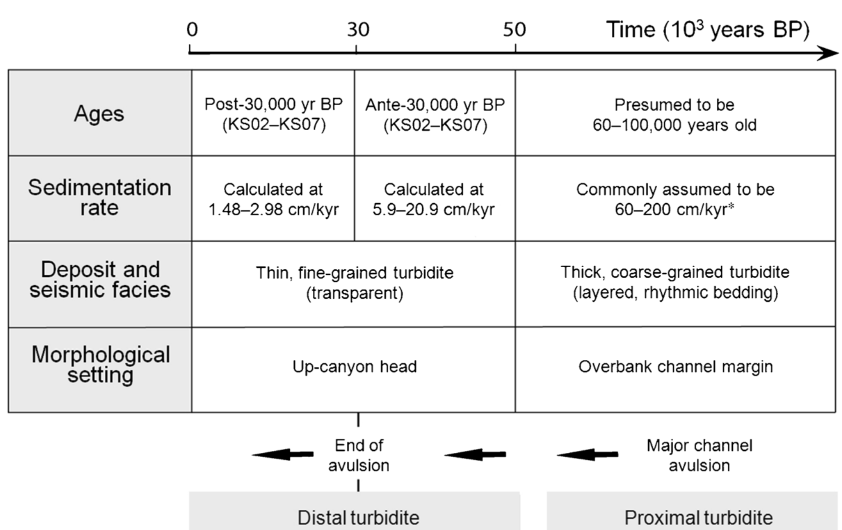

fragments and dark Jurassic limestone clasts lined by white carbonate coatings. The black plant fragments probably resulted from the reworking of relict coastal (lagoonal) deposits along the shelf break. During sea-level lowstands, these gravity-induced processes may have contributed to the observed slight acceleration in the sedimentation rates. It would seem that the gravity events were not related to any specific climatic or eustatic episodes. The distribution of gravity-process markers in the two cores suggests that site KS07 was somewhat less affected by such processes than site KS02.

General hydro-sedimentary conditions

Stanley (1981) introduced the descriptive term “unifites” to describe structureless or faintly laminated, and often thick mud layers revealing a fining-upward trend. In the Mediterranean such mud layers have been recorded in cores from the Western Alboran Basin (Huang and Stanley 1972), the Corsican Trough (Stanley et al. 1980) and the Hellenic Trench (Vittori 1978; Stanley and Maldonado 1981). Water depth does not appear to be a controlling factor because structureless mud has been collected at <1,000 m in the Corsican Trough and >4,000 m in the Hellenic Trench basins. Structureless muds, called homogenites by Kastens and Cita (1981), are essentially identical to unifites in their structural, textural and acoustic character but are restricted to small basins of the Calabrian region (western Mediterranean). Other occurrences of unifites have been reported from the western equatorial Atlantic and intraslope basins of the north-western Gulf of Mexico (Behrens 1984-1985). Off Sardinia, various depositional features in cores KS02 and KS07 are similar to unifites, especially to those of the Corsican trough. However, the high proportions of silt- and sand-size planktonic tests result in a higher planktonic/terrigenous matter ratio than observed in unifites. Moreover, unifites have typically been deposited quite rapidly (generally >200 cm/10^3 years).

In addition, the sedimentary facies of the two cores do not reveal any substantial current influence; neither is there any evidence of seafloor erosion and of vigorous sediment transport, nor alternating resuspension, winnowing and redeposition events induced by periodically intensified slope counter-currents as postulated for unifites (Stanley 1981). On the contrary, the deposits are generally structureless or, at most, faintly laminated. As cores KS02 and KS04 were collected on the southern side of the Gonone canyon head, the elevated location and distance from the main terrestrial drainage system evidently prevent particle advection associated with major gravity processes occurring in the Gonone-Orosei canyon system as a whole.

Characterization of terrigenous inputs

The terrigenous fraction of the sediments in the southern Mediterranean is the sum of atmospheric dust and eroded material transported to the sea by rivers. The atmospheric input is mainly related to windborne Saharan dust masses reaching the study area (Weldeab et al. 2005; Moreno et al. 2006; Martín-Puertas et al. 2010), and is also responsible for the enrichment of the sediment with heavy minerals (rutile and zircon; Guieu and Thomas 1996). Accordingly, Romero et al. (2008) used the Ti/Ca ratio as a proxy for the wind strength off Mauretania. In the present case, the KS02–KS07 cores show only minor variations in titanium content, which appears to be inconsistent with the stronger changes observed for other oceanic and terrigenous proxies. In the southern part of the Mediterranean Sea, increases in Saharan wind activity were assumed to have taken place during drier periods (MIS 2), but in spite of the low sediment accumulation, such increases do not seem to have had any effect in the study region, at least not on the scale of the <2 μm sub-fraction. As in the case of the shelf off Senegal (Nizou et al. 2010), major elements (Al, Fe, Ti, Si, K) can also not be considered indicative of dust input to the study area.

To this day, there have not been any specific studies dealing with the geochemical characteristics of the Quaternary deposits of the Sardinian margin. However, with respect to potential aeolian or riverine origins of the sediment, the continental margins of Mauretania and Senegal constitute relatively good comparative examples in distinguishing between alternating wet and dry periods. Thus, off Cape Ghir (southern Morocco), Kuhlmann et al. (2004) used potassium (K) contents derived from illite-mica as a fluvial proxy, whereas Caquineau et al. (2002) interpreted the same element as a dust proxy, as did Hanebuth and Lantzsch (2008) off Mauretania. Along the Senegal margin (Nizou et al. 2010), a region receiving both aeolian and fluvial supply, K is predominantly derived from potassium-feldspar and only to a minor extent from illite-mica and, as a consequence, cannot be considered as a specific proxy. Other terrigenous elements suitable as fluvial proxies are Al and Fe. However, due to the ultimate mobility of Fe, only Al has been used as a palaeoclimatic proxy along the coast of Senegal. In the study area, cores KS02 and KS07 show no major upcore change in particle source proxies, the vertical trend of the major elements considered to be indicative of terrigenous supply following a clearly opposing trend to that of the planktonic carbonates. Especially titanium, an element independent of the other constituents, shows only very small upcore variations.

Core intervals with high C/N ratios and Corg contents suggest reworking of mature organic matter from relict lowstand coastal deposits at the shelf break, being probably of lagoonal origin as observed in various other Mediterranean settings (Leclaire 1972; Giresse et al. 2009). Such reworking events must be conceived as discrete gravity processes which cannot be compared with active terrigenous supply, the events occurring indifferently and independently of the sea-level position.

As pointed out above, the only major sediment source in the study area is the Cedrino River, the suspended load of which is negligible and the bedload confined to the coast. The slope sediments, on the other hand, are mainly composed of quartz, substantial amounts of plagioclase and K-feldspar, and clay minerals (chlorite and illite), all of which are of terrigenous origin, as well as biogenic carbonates of marine origin (unpublished data). The K/Al ratios of the cores, however, do not indicate any variations suggesting a significant change in particle sources. Mg-chlorite is especially abundant and Mg enrichment (Mg/Al) has therefore been suggested to represent a good detrital proxy (Jimenez-Espejo et al. 2007). The core records, however, show that the low MgO contents are linked to the carbonates, having probably been derived from *Lithothamnium* and occasional echinoid fragments composed of high-Mg calcite.

In conclusion, even in the most favourable accumulation zones of this canyon system, terrigenous input in general remained rather modest over the last 60,000 years. This is confirmed by a shallow-seismic survey which showed the presence of only a 20–30-m-thick deposit within the deeper canyon channel with signs of very restricted progradation (Orrù and Ulzega 1987).

Sediment dynamics on the narrow Gonone shelf

In a global context, the Gonone shelf is very narrow and relatively steep, such characteristics having often been associated with sediment-starved conditions in other regions (e.g. Flemming 1981; Green 2009). One explanation of sediment starvation is linked to transgressive erosion as shorelines migrate landwards across continental shelves. Reworking of the seabed is more intense in the case of steep shelf gradients because slow shoreline displacement results in prolonged local wave action during ravinement (Davis and Clifton 1987; Cattaneo and Steel 2003). However, on the Gonone shelf, there is no evidence of seabed erosion such as remnants of beachrock/aeolianites observed on other steep shelves (e.g. Cawthra et al. 2012).

Tectonically active continental margins are often characterized by small mountainous rivers carrying large sediment loads for which there is only limited accommodation space on the narrow shelves, much of the sediment being directly transferred to the adjacent continental slopes (Milliman and Syvitski 1992). In other cases, such as off central Vietnam (South China Sea) where the narrow shelf receives large seasonal sediment inputs from the adjacent mountainous hinterland (Schimanski and Stattegger 2005; Szczuciński et al. 2009), the sedimentation rate may be high, although significant amounts still bypass the shelf as indicated by fluid-mud transport across the shelf or evidence for slumping along the shelf break. Similarly, along the narrow transform margin of southeast Africa, the occurrence of mud lenses is indicative of episodic deposition from turbid flood waters (Cawthra et al. 2012). In high-latitude and tectonically active settings, sediment supply to canyon heads is observed during falling stages, lowstands as well as sea-level highstands (Armitage and Covaut 2010).

As a rule, low progradation rates are symptomatic of low sediment supply. However, low progradation rates may also result from high sediment bypassing to deepwater sinks without accretion along the margin (Carvajal et al. 2009). Thus, the Poverty Bay shelf located on the tectonically active margin of New Zealand has evolved from a shelf with a high trapping efficiency to a system in which much of the riverine sediment bypasses the shelf because the sediment load exceeds the tectonically produced accommodation space (Miller and Kuehl 2009).

In summary, over the last 60,000 years the Sardinian margin around the Gonone Canyon has been characterized by low sedimentation rates due to the very low terrigenous inputs during both sea-level lowstand and highstand periods. The chronically slow sediment accumulation earmarks both the continental shelf and the upper slope. Both areas are mostly bypassed by any fine-grained material occasionally supplied to the shelf. As a consequence, the downslope turbidite architecture of the Gonone-Orosei system is predominantly characterized by erosional slope conduits.

Evidence for gravity-induced accumulation

The triggering mechanism of sedimentary gravity flows are either catastrophic earthquakes, moderate to large episodic floods, or frequent hyperpycnal flows which have a large impact on the geometry and internal organization of deep-sea depositional bodies as, for example, observed in the Gulf of Mexico (Weimer and Davis 1996; Weimer and Slatt 2005). Due to the scarcity and modesty of the rivers draining the island of Sardinia along its east coast, and in spite of the severity of some of the Cedrino River floods, the occurrence of flood-generated gravity flows can be discounted. This is also supported by the existence of distinct pro-delta deposits which are restricted to the nearshore shelf. On the other hand, even if the tectonic activity of Sardinia has declined since the end of the Pliocene (Antonioli et al. 1999), recent observations suggest that local seismic events still occur today (Ferranti et al. 2006; Coltorti et al. 2010). In the outer part of the shelf, the mud and fine sand cover tends to diminish and shows signs of gravity deformation of the creep-and-slump type. Also, mud deposited on the upper slope is subject to gravity-induced movement in the direction of the axial part of the canyons where the deposits can reach 30 m in thickness (Orrù and Ulzega 1987).

On the scale of the late Pleistocene, high-resolution seismic records show the presence of a bedded facies which probably indicates accumulation in the form of recurring coarse-grained turbidite sequences. This implies that, during the last few hundred–thousand years, the canyon drainage system was markedly different from the present one, which is today sheltered from major gravity mechanisms.

On a shorter timescale as that recorded in cores KS02 and KS07, additional minor modification of the canyon probably took place by local channel avulsion which succeeded in further isolating the area from major gravity processes affecting the axial part of the canyon. This isolation must have occurred at about 35,000 years BP because both cores show a simultaneous drop in the sedimentation rate by a factor of 3 at this time (Fig. 12). This coincides with evidence for reduced turbidite deposition, which can only be recognized by faint colour differences in association with an intensification of the terrigenous signal, in particular caused by the incorporation of relict sediments eroded from the outer shelf. A higher rate of plankton or siliciclastic accumulation would probably have masked this feature entirely.

Conclusions

Both study sites experienced very slow sedimentation, the rate decreasing from the MIS III (20 cm/10^3 years) towards the MIS II and I (3 cm/10^3 years), this being the most remarkable result of the study. As sedimentation rates on this scale preclude global climatic controls, a number of other explanations are proposed on the basis of the modern oceanic conditions along the eastern Sardinian continental margin:

– terrigenous supplies are modest, the silty-sandy Cedrino pro-delta extending seawards over only 1 km and seawaters showing an exceptional transparency which enhances photosynthetic production; erosion of Jurassic limestones, which constitute most of the bedrock of the shelf and the shoreline, only supply very small amounts of suspended material to the sea;
– as a consequence, strong biogenic carbonate accumulation prevails both on the shelf (benthic accumulation), where it masks the relict deposits of the last sea-level lowstand, and on the adjacent slope (pelagic accumulation);
– planation of the deposits may have occurred, although there is no evidence for truncation (e.g. a sharp upper contact or sedimentary gap) throughout the homogeneous core deposits;
– the impact of minor sediment gravity flows, probably originating at the shelf break, is evident in the sedimentary and geochemical balance, being particularly well highlighted by occasional peaks in organic matter contents (high C/N ratios);
– the homogeneity of major elements throughout the cores, in particular of titanium, strengthens the notion of low terrestrial contributions, although sedimentation was slightly higher during MIS III, suggesting that the head of the Gonone Canyon underwent morphologic evolution leading to progressive shelter from major gravity processes affecting other parts of the canyon system;
– local seismic instability still prevails and initiates gravity deformations of the creep-and-slump type, and causes mud deposition in the axial part of the canyon.

Acknowledgements The METYSS cruises as well as the laboratory analyses were supported by the French “ACTIONS MARGES” and “ACTION COORDONNEE” INSU programs. We warmly thank the captains of the R/V Téthys II (INSU/CNRS), Rémi Lafond and Joël Le Guennec, and their crews for their participation in data acquisition offshore. The study has been performed according to the Russian Government Program of Competitive Growth of Kazan Federal University to V. Pascucci. We also wish to acknowledge Andrew Green and Mauro Coltorti for their critical reading of the original manuscript, as well as the editors Burg Flemming and Monique Delafontaine for their helpful comments. Gary Fowler helped us with the English language.

References

Antonioli F, Silenzi S, Vittori E, Villani C (1999) Sea level changes and tectonic mobility: precise measurements in three coastlines of Italy considered stable during the last 125 ky. Phys Chem Earth 24(4): 337–342

Armitage DA, Covaut JA (2010) “Exceptional” turbidite systems in high latitude and tectonically active settings and the obsolescence of ubiquitous sequence stratigraphic models. AAPG Convention, 11–14 April 2010, New Orleans, LA, Abstract #90104

Beccaluva L, Deriu M, Macciotta G, Savelli G, Venturelli G (1977) Geochronology and magmatic characters of the Pliocene-Pleistocene volcanism in Sardinia (Italy). Bull Volcanol 40:154–168

Beccaluva L, Civetta L, Macciotta G, Ricci CA (1985) Geochronology in Sardinia: results and problems. Ren Soc It Mineral Petrol 40:57–72

Behrens EW (1984–1985) Unifite muds in intraslope basins, northwest Gulf of Mexico. Geo-Mar Lett 4:227–233. doi:10.1007/BF02281711

Berné S, Jouet G, Bassetti MA, Dennielou B, Taviani M (2007) Late Glacial to Preboreal sea-level rise recorded by the Rhône deltaic system (NW Mediterranean). Mar Geol 245:65–88

Calvert SE (1976) The mineralogy and geochemistry of near-shore sediments. In: Riley JP, Chester R (eds) Chemical Oceanography, vol 6. Academic Press, London, pp 187–280

Caquineau S, Gaudichet A, Gomes L, Legrand M (2002) Mineralogy of Saharan dust transported over northwestern tropical Atlantic Ocean in relation to source regions. J Geophys Res Atmos 107(D15):AAC 4-1–AAC 4-12

Carminati ER, Wortel W, Spakman W, Sabadini R (1998) The role of slab-detachment processes in the opening of the western-central Mediterranean basins: some geological and geophysical evidence. Earth Planet Sci Lett 160:651–665

Carobene L (1978) Valutazione di movimenti recenti mediante ricerche morfologiche su falesie e grotte marine del Golfo di Orosei. Mem Soc Geol Ital 19:641–649

Carvajal C, Steel R, Pettern A (2009) Sediment supply: the main driver of shelf margin growth. Earth Sci Rev 79(9):652–672

Cattaneo A, Steel RJ (2003) Transgressive deposits: a review of their variability. Earth-Sci Rev 62:187–228

Cawthra HC, Neumann FH, Uken R, Smith AM, Guastella L, Yates A (2012) Sedimentation on the narrow (8 km wide), oceanic current-influenced continental shelf off Durban, KwaZulu-Natal, South Africa. Mar Geol 323–325:107–122

Chanier F, Reynaud JY, Gaullier V, Maillard A, Thinon I, Lymer G, Giresse P, Bassetti MA, Lofi J (2011) Contrôle de l'enregistrement stratigraphique du Pliocène sur la côte est-sarde: effets de la Crise de Salinité Messinienne ou tectonique post-rift? In: Livre des résumés, 13th Congress of French Sedimentologists (ASF), 14–16 November 2011, Dijon. Publ ASF, Paris, p 78

CIESM/Ifremer Medimap Group (2008) Morpho-bathymetry of the Mediterranean Sea. CIESM, Monaco

Coltorti M, Melis E, Patta D (2010) Geomorphology, stratigraphy and facies analysis of some Late Pleistocene and Holocene key deposits along the coast of Sardinia (Italy). Quat Int 222(1–2):19–35

Cossu A, De Waele J, Francesco Sanna F, Sanna L (2014) Preliminary estimation of the peak discharge at the Su Gologone spring (Central-East Sardinia) during the flood event of November 18th, 2013. Geophys Res Abstr16, EGU2014-15708

Dalla Valle G (2007) Dinamica sedimentaria torbiditica in bacini confinati: margine orientale della Sardegna. Doctoral thesis, University of Bologna, Italy

Dalla Valle G, Gamberi F (2010) Erosional sculpting of the Caprera confined deep-sea fan as a result of distal-spilling processes (eastern Sardinian margin, Tyrrhenian sea). Mar Geol 268:55–66

Dalla Valle G, Gamberi F, Rocchini P, Minisini D, Errera A, Baglioni L, Trincardi F (2013) 3D seismic geomorphology of mass transport complexes in a foredeep basin: examples from the Pleistocene of the Central Adriatic Basin (Mediterranean Sea). Sed Geol 294:127–141

Davis RA, Clifton HE (1987) Sea-level change and the preservation potential of wave-dominated and tide-dominated coastal sequences. In: Nummedal D, Pilkey OH, Howard JD (eds) Sea-level fluctuation and coastal evolution. SEPM Spec Publ 41:167–178

Dewey JF, Helman ML, Turco E, Hutton DHW, Knott SD (1989) Kinematics of the western Mediterranean. In: Coward MP, Dietrich D, Park RG (eds) Alpine tectonics. Geol Soc Lond Spec Publ 45:265–283

Droxler AW, Schlager W (1985) Glacial versus Interglacial sedimentation rates and turbidite frequency in the Bahamas. Geology 13:799–802

Ferranti L, Antonioli F, Mauz B, Amorosi A, Dai Pra G, Mastronuzzi G, Monaco G, Orrù P, Pappalardo M, Radtke U, Renda P, Romano P, Sansò P, Verrubbi B (2006) Markers of the last interglacial sea-level highstand along the coast of Italy: tectonic implications. Quat Int 145–146:30–54

Flemming BW (1981) Factors controlling shelf sediment dispersal along the south-east African continental margin. Mar Geol 42:259–277

Gamberi FG, Dalla Valle G (2009) The impact of margin shaping processes on the architecture of the Sardinian and Sicilian margin submarine depositional systems within the Tyrrhenian Sea. SEPM Spec Publ 92:207–219

Gaullier V, Chanier F, Lymer G, Vendeville BC, Maillard A, Thinon I, Lofi J, Sage F, Loncke L (2014) Salt tectonics and crustal tectonics along the Eastern Sardinian margin, Western Tyrrhenian: new insights from the "METYSS 1" cruise. Tectonophysics 615–616:69–84

Giresse P, Pauc H, Déverchère J, Maradja Shipboard Scientific Party (2009) Sedimentary processes and origin of sediment gravity-flow deposits on the western Algerian margin during late Pleistocene and Holocene. Mar Petrol Geol 26:695–710

Giresse P, Bassetti MA, Chanier F, Maillard A, Reynaud J-Y, Gaullier V, Lymer G, Lofi J, Thinon F (2011) Les dépôts marins et continentaux pliocènes de la côte orientale de la Sardaigne (secteur d'Orosei) dans le cadre de l'évolution morphostructurale de la région. In: Livres des résumés, 13th Congress of French Sedimentologists (ASF), 11–15 November 2011, Dijon. Publ ASF, Paris, p 155

Giresse P, Bassetti M-A, Pauc H, Gaullier V, Déverchère J, Bracene R, Yelles A (2013) Sediment accumulation rates and turbidite frequency in the eastern Algerian margin. An attempt to examine the triggering mechanisms. Sed Geol 294:266–281

Grantz A, Phillips RL, Mullen MW, Starratt SW, Jones GA, Naidu AS, Finney BP (1996) Character, paleoenvironment, rate of accumulation, and evidence of seismic triggering of Holocene turbidites, Canada Abyssal Plain, Arctic Ocean. Mar Geol 133:51–73

Green AN (2009) Sediment dynamics on the narrow, canyon-incised and current swept shelf of the northern KwaZulu-Natal continental shelf, South Africa. Geo-Mar Lett 29:201–219. doi:10.1007/s00367-009-0135-9

Guieu C, Thomas A (1996) Saharan aerosol: from the soil to the ocean. In: Guerzoni S, Chester R (eds) The impact of desert dust across the Mediterranean. Kluwer, Dordrecht, pp 207–216

Hanebuth TJJ, Lantzsch H (2008) A Late Quaternary sedimentary shelf system under hyperarid conditions: unravelling climatic, oceanographic and sea-level controls (Golfe d'Arguin, Mauritania, NW Africa). Mar Geol 256:77–89

Huang TC, Stanley DJ (1972) Western Alboran Sea: sediment dispersal, ponding and reversal of currents. In: Stanley DJ (ed) The Mediterranean Sea: a natural sedimentation laboratory. Dowden, Hutchinson & Ross, Stroudsburg, PA, pp 521–559

Imbrie J, Hays JD, Martinson DG, McIntyre A, Mix AC, Morley JJ, Pisias NG, Prell WL, Shackleton NJ (1984) The orbital theory of Pleistocene climate: support from a revised chronology of the marine $\delta^{18}O$ record. In: Berger A, Imbrie J, Hays H, Kukla G, Saltzman B (eds) Milankovitch and climate: understanding the response to astronomical forcing. Proc NATO Advanced Research Worksh, 30 November–4 December 1982, Palisades, NY. D Reidel, Dordrecht, pp 269–305

Jimenez-Espejo FJ, Martinez-Ruiz F, Sakamoto T, Iijima K, Gallego-Torres D, Harada N (2007) Paleonvironmental changes in the western Mediterranean since the last glacial maximum: high resolution multiproxy record from the Algero-Balearic basin. Palaeogeogr Palaeoclimatol Palaeoecol 246:292–306

Jouet G, Berné S, Rabineau M, Bassetti MA, Bernier P, Dennielou B (2006) Shoreface migrations at the shelf edge and sea-level changes around the Last Glacial Maximum (Gulf of Lions, NW Mediterranean Sea). Mar Geol 234:21–42

Kastens KA, Cita MB (1981) Tsunami induced sediment transport in the abyssal Mediterranean Sea. Geol Soc Am Bull 89:591–604

Kastens KA, Mascle J, Auroux C (1987) Proceedings of the Ocean Drilling Program, Part A. Initial Reports, Sites 650–656, 107. Ocean Drilling Program, College Station, TX

Kuhlmann H, Meggers H, Freudenthal T, Wefer G (2004) The transition of the monsoonal and the N Atlantic climate system off NW Africa during the Holocene. Geophys Res Lett 31, L22204. doi:10.1029/2004GL021267

Lambeck K, Bard E (2000) Sea-level changes along the French Mediterranean coast for the past 30,000 years. Earth Planet Sci Lett 175:203–222

Lambeck KF, Antonioli A, Purcell S, Silenzi S (2004) Sea level change along the Italian coast from the past 10,000 yr. Quat Sci Rev 23:1567–1598

Leclaire L (1972) La sédimentation holocène sur le versant méridional Algéro-Baléares (Précontinent algérien). Mém Mus Natl Hist Paris CXXIV:1–392

Lofi J, Sage F, Déverchère J, Loncke L, Maillard A, Gaullier V, Thinon I, Gillet H, Guennoc P, Gorini C (2011) Refining our knowledge of the Messinian salinity crisis records in the offshore domain through multi-site seismic analysis. Bull Soc Géol Fr 182(2):163–180

Lo Iacono C, Guillen J, Puig P, Ribo M, Ballesteros M, Palanques A, Farran M, Accosta J (2010) Large-scale bedforms along a tideless outer shelf setting in the western Mediterranean. Cont Shelf Res 30: 1802–1813

Lustrino M, Melluso L, Morra V (2002) The transition from alkaline to tholeiitic magmas: a case study from the Orosei-Dorgali Pliocene volcanic district (NE Sardinia, Italy). Lithos 63(1–2):83–113

Mariani P, Braitenberg C, Antonioli F (2009) Sardinia coastal uplift and volcanism. Pure Appl Geophys 166:1369–1402

Martín-Puertas C, Jiménez-Espejo F, Martínez-Ruiz F, Nieto-Moreno V, Rodrigo M, Mata MP, Valero-Garcés BL (2010) Late Holocene climate variability in the southwestern Mediterranean region: an integrated marine and terrestrial geochemical approach. Clim Past 6:807–816

Martini IP, Andreucci I, Pascucci V (2009) Slope deposits of the calcareous coastal hills along the Gulf of Orosei, NE Sardinia - karstic and periglacial influence. In: IAS, Abstract Book, 27th Regional Meeting of Sedimentologists, 20–23 September 2009, Alghero, Italy, p 596

Mascle J, Réhault JP (1990) A revised seismic stratigraphy of the Tyrrhenian Sea: implications for the basin evolution. In: Kastens KA, Mascle J et al., Proc Ocean Drill Program Sci Res 107:617–636

Miller AJ, Kuehl SA (2009) Shelf sedimentation on a tectonically active margin: a modern sediment budget for Poverty continental shelf, New Zealand. Mar Geol 175:175–187

Milliman JD, Syvitski JPM (1992) Geomorphic/tectonic control of sediment discharge to the ocean: the importance of small mountainous rivers. J Geol 100:525–544

Moreno T, Querol X, Castillo S, Alastuey A, Cuevas E, Herrman L, Mounkaila M, Elvira J, Gibbons W (2006) Geochemical variations of aeolian mineral particles from the Sahara-Sahel dust corridor. Chemosphere 65:261–270

Nizou J, Hanebuth TJJ, Heslop D, Schwenk T, Palamenghi LK, Stuut J-B, Henrich R (2010) The Senegal River mud belt: high-resolution archive of paleoclimatic change and coastal evolution. Mar Geol 278:150–164

Orrù P, Ulzega A (1987) Rilevamento geologico e geomorfologico costiero e sottomarino applicato alla definizione delle risorse ambientali (Gollfo di Orosei, Sardegna Orientale). Mem Soc Geol It 37:471–479

Palanques A, Puig P, Guillén J, Jiménez J, Gracia V, Sánchez-Arcilla A, Ma O (2002) Near-bottom suspended sediment fluxes on the microtidal low-energy Ebro continental shelf (NW Mediterranean). Cont Shelf Res 22(2):285–303

Pascucci V, Merlini S, Martini IP (1999) Seismic stratigraphy of the Miocene-Pleistocene sedimentary basins of the Northern Tyrrhenian Sea and western Tuscany (Italy). Basin Res 11: 337–356

Pascucci V, Andreucci S, Sanna L, Capucci S, Orrù PE (2014) Note illustrative della Carta Geologica d'Itali alla scala 1/50.000, Foglio 500 Nuoro Est. Servizo geologico d'Italia, Istituto Superior per la Protezione e la Ricerca Ambientale, Rome

Patacca E, Sartori R, Scandone P (1990) Tyrrhenian basin and Apenninic arcs: kinematic relations since Late Tortonian times. Mem Soc Geol It 45:425–451

Pichevin L, Mulder T, Savoye B, Gervais A, Cremer M, Piper DJW (2003) The Golo submarine turbidite system (east Corsica margin): morphology and processes of terrace formation from high-resolution seismic reflection profiles. Geo-Mar Lett 23:117–124. doi:10.1007/s00367-003-0131-4

Romero OE, Kim J-H, Donner B (2008) Submillennial-to-millennial variability of diatom production off Mauritania, NW Africa, during the last glacial cycle. Paleoceanography 23, PA3218. doi:10.1029/2008PA001601

Sartori R, Carrara G, Torelli L, Zitellini N (2001) Neogene evolution of the southwestern Tyrrhenian Sea (Sardinia basin and western bathyal plain). Mar Geol 175:47–66

Schimanski A, Stattegger K (2005) Deglacial and Holocene evolution of the Vietnam shelf: stratigraphy, sediments and sea-level change. Mar Geol 214:365–387

Stanley DJ (1981) Unifites: structureless muds of gravity-flow origin in Mediterranean basins. Geo-Mar Lett 1:77–83. doi:10.1007/BF02463322

Stanley DJ, Maldonado A (1981) Depositional models for fine-grained sediment in the Western Hellenic Trench, eastern Mediterranean. Sedimentology 28:273–290

Stanley DJ, Rehault J-P, Stuckenrath R (1980) Turbid-layer bypassing model: the Corsican Trough, northwestern Mediterranean. Mar Geol 37:19–40

Szczuciński W, Stattegger K, Scholten J (2009) Modern sediments and sediment accumulation rates on the narrow shelf off central Vietnam, South China Sea. Geo-Mar Lett 29:47–59. doi:10.1007/s00367-008-0122-6

Urgeles R, Cattaneo A, Puig P, Liquete C, Ben De Mol DA, Sultan N, Trincardi F (2011) A review of undulated sediment features on Mediterranean prodeltas: distinguishing sediment transport structures from sediment deformation. Mar Geophys Res 32(1–2):49–69

Vittori J (1978) Caractères structuro-sédimentaires de la couverture plio-quaternaire au niveau des pentes et des fosses helléniques du Peloponnèse. Doctoral thesis, University of Perpignan, France

Weimer P, Davis TL (1996) Applications of 3-D seismic data to exploration and production. Studies in Geology, vol 42. AAPG, Tulsa, OK

Weimer P, Slatt RM (2005) Petroleum systems of deep-water settings. EAGE/SEG Distinguished Instructor Short Courses, vol 7. European Association of Geoscientists and Engineers (EAGE), Houten, The Netherlands

Weldeab S, Schneider RR, Kölling WG (2005) Holocene African droughts relate to eastern equatorial Atlantic cooling. Geology 33: 981–984

Wetzel A (1984) Bioturbation in deep-sea fine-grained sediments: influence of sediment texture, turbidite frequency, and rates of environmental change. In: Stow DAW, Piper DJW (eds) Fine-grained sediments: deep-water processes and facies. Geol Soc Lond Spec Publ 15:595–608